

1. Introduction

The growing demand for cooking oil in the expanding food and beverage industry has resulted in greater waste production, which significantly contributes to oil pollution. Waste cooking oil contains harmful substances, including carcinogenic polycyclic aromatic hydrocarbons, that pose a risk to water sources. Improper disposal methods, especially pouring used oil down drains, often result in solidification and blockage of sewage systems, causing serious obstructions. Additionally, water contamination has become a critical concern globally, with industrial wastewater, domestic sewage, and oil leakage contributing to environmental degradation. These environmental and health risks underscore the urgent need for improved waste management practices to address the global challenge of oil pollution. Failure to manage this issue may lead to catastrophic consequences for ecosystems and contribute to climate change [1-4].

Therefore, it is crucial to develop innovative and practical methods to reduce the harmful effects of oil contamination. While various techniques have been designed to address this issue, they are often challenging to implement at contaminated sites, costly, and may produce unwanted by-products [5]. Various methods are utilized to manage cooking oil waste, such as biodiesel production, thermal decomposition, flotation [6] gravitational separation [7] membrane filtration [8,9] and the use of sorbent materials [4]. However, these conventional methods are generally ineffective, lack selectivity, and incur high operating costs [1]. Among these, oil-water separation being the most widely utilized technique. Therefore, it is necessary to develop new functional materials that can selectively and efficiently absorb or separate oil from oily wastewater. In this regard, superhydrophobic materials featuring contact angles (CA) in water higher than 150° have been intensively researched and manufactured for achieving an efficient oil/water separation [10]. Recent studies emphasize the effectiveness of superhydrophobic cellulose beads for selective oil absorption, attributed to their microporous, hydrophobic structure [1,10].

Recently, significant research attention has focused on using natural fibers for the remediation of polluted water [5]. Sugarcane bagasse has been shown to remove up to 70% of hydrocarbons from polluted water [11]. Other natural fibers, such as straw-peat composites, and agricultural wastes like rice straw, activated rice husk, and naturally hydrophobic cellulose, have also proven effective in hydrocarbon removal [5,8]. Cellulose, the most abundant biopolymer found on Earth, holds immense value as an invaluable, renewable, biodegradable, and bio-compatible energy source. The cell wall of lignocellulosic plants primarily consists of cellulose, whose composition varies depending on factors such as plant species, environmental conditions, growth location, and maturity stage [12]. Each cellulose unit has three distinct hydroxyl groups (-OH) found on carbons 2, 3, and 6. Although it is well known that the one on carbon 6 has a significant reactivity compared to the -OH on carbons 2 and 3.

Furthermore, due to the high reactivity of the hydroxyl groups of cellulose, the modification of cellulose can be achieved chemically through a variety of reactions including sulfonation, esterification, silanation, oxidation, and etherification depending on the intended application [1,9]. However, cellulose is naturally highly hydrophilic, limiting its ability to selectively absorb oils and organic solvents from water. Hydrophobic and oleophilic materials are better suited for oil-water or hydrocarbon-water separation. This can be achieved by modifying the surface chemistry of cellulose to enhance its surface functionality [11,12].

Hence, in using absorbents for oil removal, most materials, such as silica, clay, polymers, and cellulose-based substances, are modified to enhance their oleophilic properties [4]. Hence, to create hydrophobic materials, a rough surface structure must first be established, followed by chemical modification to achieve low surface energy on the material's surface [1]. In many cases, organosilanes

are an ideal choice for surface modification. Silanes can be grafted onto material surfaces through chemical vapor deposition, altering the interaction between solid surfaces and water. Previous studies have shown that various cellulose-based materials can reduce hydrophilicity by crosslinking hydroxyl groups with silanes [1,12,13].

Therefore, this study aims to synthesize regenerated cellulose beads, which are then converted into cellulose aerogel microbeads through freeze-drying process to create a porous structure that facilitates oil absorption. Subsequently, the cellulose aerogel microbeads was underwent silanation using trimethoxymethylsilane (TMMS) as the silane agent. The samples were characterized and analyzed for their chemical and thermal properties using Attenuated Total Reflectance-Fourier Transform Infrared (ATR-FTIR) spectroscopy and thermogravimetric analysis (TGA), respectively. Meanwhile, hydrophobicity of the silanated cellulose aerogel microbeads was measured using contact angle measurement. The oil-water separation was also being investigated through oil retention test in water.

2. Methodology

2.1 Materials

The primary material utilized in this study was cellulose derived from natural cellulose extracted from cotton. The cellulose fiber was procured from Multifilla (M) Sdn. Bhd. in Malaysia. In the production of the cellulose solvent, sodium hydroxide pellets and urea were employed, sourced from R&M Chemicals and HmBG Chemicals, respectively. The regeneration process involved the use of hydrochloric acid (HCl), 37% as a coagulant for microbeads preparation and was purchased from R&M Chemicals. The silanation process utilized Trimethoxymethylsilane (TMMS) 98%, and anhydrous ethanol served as the solvent where both acquired from Sigma Aldrich. Meanwhile, used cooking oil used was gathered from households.

2.2 Preparation of Cellulose Aerogel Microbeads (CAM)

Green cellulose solvent was prepared prior to the dissolution of cellulose containing 7% NaOH and 12 % urea subsequently and pre-cooled in refrigerator overnight and the temperature dropped to -20 °C. The frozen solvent was thawed until the solvent reached -13 °C before adding 4% cellulose to the pre-cooled solvent and vigorously stirred at high-speed using a mechanical stirrer until complete dissolution of the cellulose occurred, resulting in the formation of a cellulose solution. Consequently, the cellulose solution was injected into a 5% H₂SO₄ coagulant to form beads. This process effectively creates cellulose microbeads using a dropping technique for subsequent applications. The formed microbeads were allowed to regenerate in the solution for 12 hours before washing for solvent exchange and subsequent freeze-drying, porous spherical cellulose beads were produced. These beads were filtered, washed, neutralized, and finally freeze-dried to produce cellulose aerogel microbeads (CAM) with porous structure, which was stored in a sealed container for later use.

2.3 Silanation of Cellulose Aerogel Microbeads

Trimethoxymethylsilane (TMMS) solution of 5 % were prepared by diluting TMMS in anhydrous ethanol as TMMS solvent. The CAM were mixed with different TMMS solutions in open glass vial in vacuum desiccator and placed on hot plate to allow heating process to occur for 3 hours incubation period at 70 °C, where the elevated temperature facilitates the silanation reaction. During this

period, silane molecules reacted with the surface functional groups of cellulose promoting the bonding of silane molecules to the cellulose surface. During this period, TMMS underwent hydrolysis and reacted with hydroxyl groups on the cellulose, forming siloxane bonds and introducing hydrophobic groups as shown in Fig. 1. Ultimately, the CAM coated with TMMS with different TMMS concentration which denoted as (3/sCAM and 5/sCAM) were subjected to a vacuum oven to eliminate excess TMMS. The silane grafting process, accomplished through chemical vapor deposition on the surfaces of CAM, enhances the interaction at the boundary layers between solids and water. The effect of CVD time on the surface modification of sCAM was investigated where the sCAM was subjected to TMMS at different interval time of 30, 60 and 120 minutes. This modification extends the functionality, specifically enhancing the surface hydrophobicity of the CAM. The summary of the sample preparation is shown in Table 1.

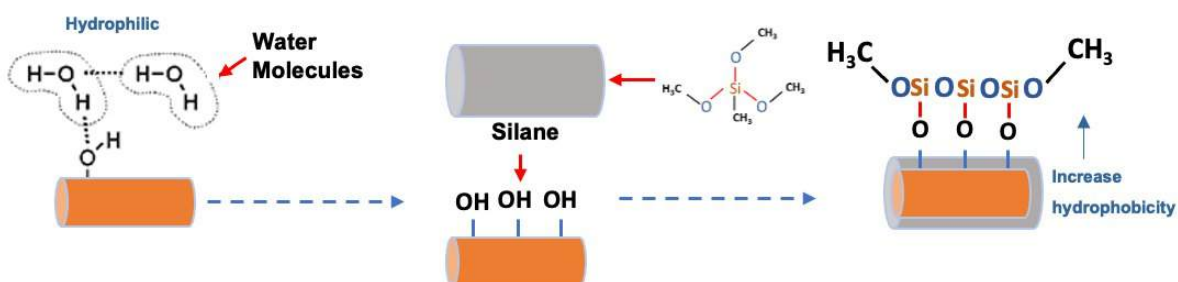


Fig. 1. Silanation of cellulose with TMMS producing siloxane bonds and increased hydrophobicity of cellulose surface

Table 1

Sample preparation

Sample's name	Concentration of TMMS (%)	CVD Time (min)
CAM	0	-
3/sCAM30	3	30
3/sCAM60	3	60
3/sCAM120	3	120
5/sCAM30	5	30
5/sCAM60	5	60
5/sCAM120	5	120

2.4 Oil Absorption Study

The oil uptake efficiency test involved a kinetic study where silanated cellulose aerogel microbeads (sCAM) were immersed in used cooking oil for different time intervals until equilibrium was reached. Each sample was then taken out at the designated times, blotted with filter paper, and weighed. Oil uptake was calculated using the formula for oil uptake percentage according Eq. 1.

$$\text{Oil Absorption Capacity (\%)} = (W_{\text{wet}} - W_{\text{dry}}) / W_{\text{dry}} \times 100 \quad (1)$$

where W_{wet} is the weight of absorbed sCAM and W_{dry} is the weight of the dried sCAM.

2.5 Pore Volume Measurement

The pore volume measurement was carried out using liquid displacement method. The silanated cellulose aerogel microbeads was dried to remove any moisture absorbed into the structure. The dried sCAM was weighted to recode the initial volume. Dried CAM then was immersed in oil and ensure it is completely saturated, allowing it to displace the liquid in a graduated cylinder. The new volume level after sCAM submerged in water was observed and recorded. The difference between the initial and final volume readings is the volume of the displaced liquid and the pore volume was calculated according to Equation 1. The volume of the displaced water represents the pore volume of the aerogel, assuming the sample's solid framework does not absorb the liquid.

$$\text{Pore Volume} = V_{\text{displaced liquid}} - V_{\text{solid aerogel}} \quad (2)$$

2.6 Characterization

The surface morphology of the samples were investigated using scanning electron microscope (SEM LEO 1450VP). The samples were sputter-coated with gold before the observation. The functional groups of cellulose, CAM and sCAM samples were investigated using attenuated total reflectance-Fourier transform infrared (ATR-FTIR) spectroscopy (ALPHA; Bruker) with a resolution of 1 cm^{-1} within the wavenumber range of $4,000$ to 650 cm^{-1} . This analysis aimed to detect changes in functional groups during the silanation process. Additionally, a thorough examination of the FTIR spectrum concentrated on identifying the presence of siloxane within the sCAM structure. Thermogravimetric analysis (TGA) was performed by changes in the thermal degradation of CAM and sCAM samples at temperatures ranging from 27 to $650 \text{ }^\circ\text{C}$ under nitrogen condition at a heating rate of $10 \text{ }^\circ\text{C}/\text{min}$.

2.7 Oil-water Separation Study

A simple oil-water separation test was performed on all silanated samples (silanated in different silanation time). Beakers were prepared and each beaker was filled with water and the other with cooking oil, engine oil and mineral oil. A small piece of hydrophobic cellulose (sCAM) was then added to each beaker. Observations were made on how the cellulose interacted with each liquid where the time it takes for the cellulose to absorb the oil, demonstrating its selectivity measured using by stopwatch and image taken by camera.

2.8 Contact Angle Measurement

The contact angle of the waste cooking oil on CAM and sCAM were measured by the Sessile Drop Method for the wettability and hydrophobicity evaluation. **Fig. 2** shows an image of the oil droplet on the samples taken by a camera. The contact angle of the oil droplet is the angle between a horizontal line and tangential line of the droplet at a contact point of an edge of the oil droplet [14].

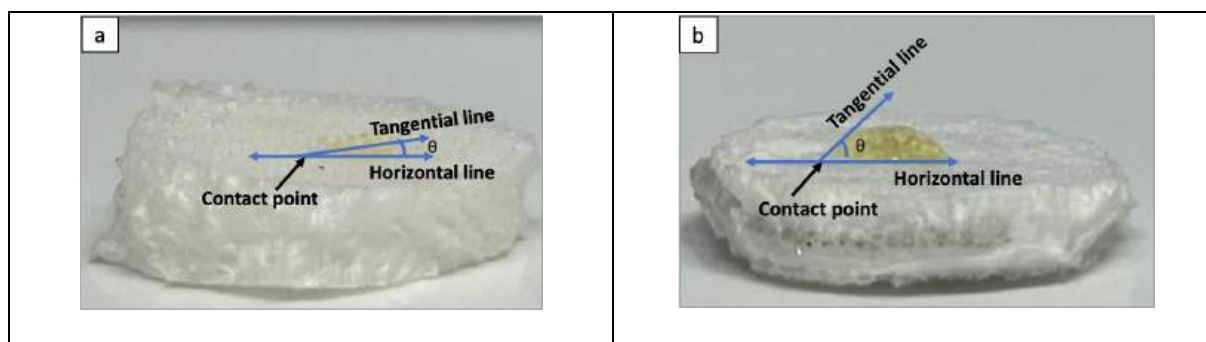


Fig. 2. Contact angle measurement of oil drop on (a) CAM and (b) sCAM

3. Results and Discussion

3.1 Porous Structure of Cellulose Microbeads

The morphological structure of cellulose and cellulose aerogel microbeads were observed by FESEM and it showed compact structure of cellulose fiber (Fig. 3(a)). Meanwhile, morphological structure of cellulose aerogel microbeads (Fig. 3(b)) showed highly porous structure of the CAM sample [15,16]. This is due to the pore formed after the cellulose beads undergo freeze drying process. In addition, during the coagulation process in HCL, solvent penetrated into the cellulose-rich phase and create pores. During the freeze drying process, the removal of solvent and water in the cellulose molecules leads to formation of porosity. The porosity observed can be attributed to the freeze-drying process, during which the formation of pores occurs as the cellulose beads undergo solvent and water removal. Additionally, during coagulation in HCl, solvent penetrated into the cellulose-rich phase which facilitates more pore generation. Consequently, the subsequent freeze-drying step promotes the development of a porous structure due to the solvent and water removal from the cellulose matrix [17-20].

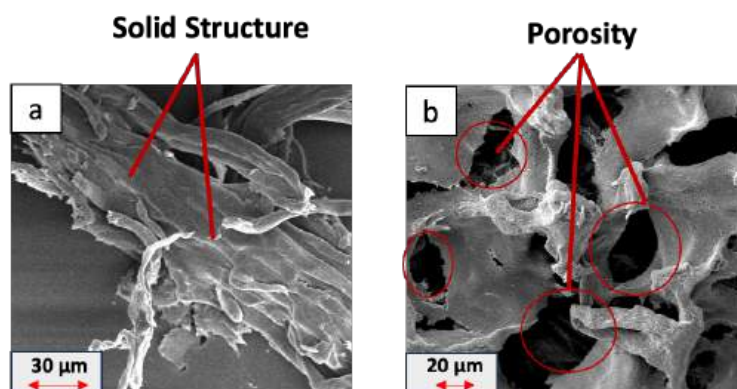


Fig. 3. SEM images of (a) cellulose and (b) cellulose aerogel microbeads

3.2 Functional Groups Studies

Fourier-transform infrared (FTIR) spectroscopy confirmed the successful silanization of cellulose aerogel microbeads (CAM) into hydrophobic sCAM. The broad O–H stretching band around 3300–3400 cm^{-1} in CAM indicates abundant hydroxyl groups, which are significantly attenuated in sCAM due to partial substitution by silane, demonstrating effective surface modification. The sCAM spectrum reveals new peaks between 1000 –1200 cm^{-1} , corresponding to Si–O–C at 1050 cm^{-1} and Si–O–Si at around 1100 cm^{-1} stretching vibrations, confirming the formation of covalent bonds and polysiloxane networks on the cellulose surface. Additionally, a minor feature around 800–850 cm^{-1}

in the sCAM spectrum is attributed to Si-CH₃ bending modes, further supporting successful grafting of alkyl-silane moieties. The persistence of the C-O stretching band (~1030 cm⁻¹) in both samples indicates that the cellulose backbone structure remains intact post-modification [19]. These spectral changes presented that the reduction in hydroxyl intensity and emergence of siloxane-specific bands provide strong evidence for the chemical transformation of CAM into sCAM.

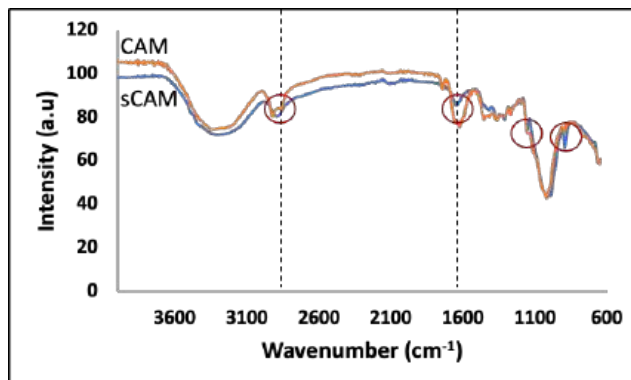


Fig. 4. FTIR spectrum of CAM and sCAM

3.3 Thermal Analysis

The thermal degradation behavior of CAM and sCAM was investigated using thermogravimetric analysis (TGA). **Fig. 5** shows the CAM and sCAM samples respond to increasing temperatures from 0 to 600 °C under thermogravimetric analysis. At the first 150 °C, the CAM samples shows degradation by 10% and sCAM has degraded by 5% of their original mass and maintained to 250 °C. Both samples exhibited an initial mass loss below 150 °C, which is attributed to the evaporation of physically adsorbed moisture and residual solvents [20-22]. CAM showed a pronounced weight loss between 250–380 °C at the second decomposition step, corresponding to the depolymerization and decomposition of cellulose chains through cleavage of glycosidic linkages and dehydration reactions [21,23].

In contrast, sCAM demonstrated a slight shift of the onset degradation temperature towards higher values, indicating improved thermal stability imparted by the silanization process [24]. The incorporation of silane groups likely forms a protective barrier and induces partial crosslinking, which delays thermal decomposition. Furthermore, the residual mass at 600 °C was higher for sCAM compared to CAM, suggesting the presence of thermally stable siloxane structures from the silane modification. These observations confirm that silanization effectively enhances the thermal resistance of cellulose aerogel microbeads [24,25].

The DTG profiles further explained these trends. Both samples displayed a minor DTG peak at ~100 °C due to moisture desorption, with sCAM showing a lower peak intensity. The major DTG peak at ~330 °C, attributed to cellulose pyrolysis, was broader and slightly shifted for sCAM, indicating a more complex degradation process. This broader profile suggests contributions from thermally stable siloxane networks, which decompose at elevated temperatures between 350–450 °C. Moreover, sCAM exhibited a higher residual mass above 500 °C, consistent with the presence of thermally resistant siloxane structures [1,25].

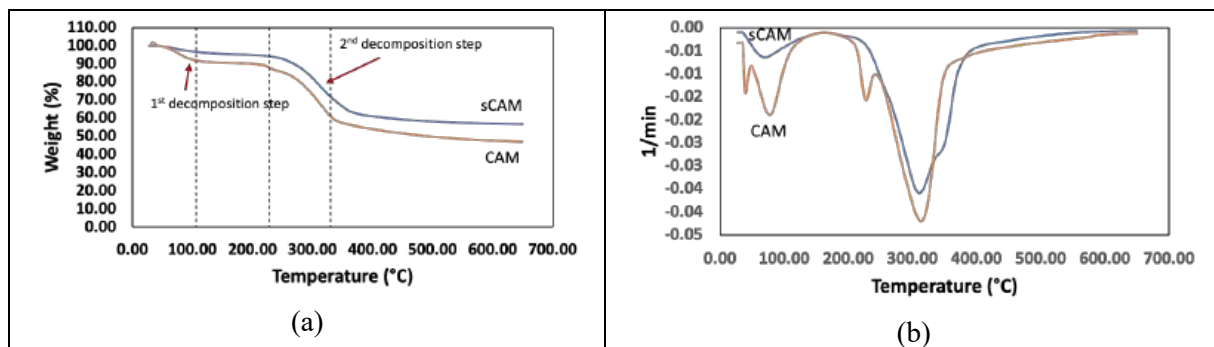


Fig. 5. (a) TGA curve and (b) DTG profiles of CAM and sCAM

3.4 Oil Absorption Study

The oil sorption performance of cellulose aerogel microbeads (CAM) and silanized aerogels (sCAM) was evaluated through measurements of oil retention capacity, pore volume, and absorption kinetics as shown in Fig. 6. The unmodified CAM sample exhibited a moderate oil retention of 543% and a pore volume of 346%. However, after silanization process, the 3/sCAM30 and 5/sCAM30 samples achieved the highest oil retention values of 560% and 822%, respectively, along with significantly enhanced pore volumes of 988% and an increase pore structure attributable to simultaneous hydrophobic surface modification and preserved porosity. However, extending silanization time between 60–120 min led to pore collapse due to excessive silane deposition which correlate to the reducing oil uptake reduce to 125% for 3/sCAM120 and pore volume due to pore obstruction. These trends were also observed in absorption kinetics where 3/sCAM30 and 5/sCAM30 rapidly reached equilibrium more 400% within 20 minutes, whereas prolonged silanization produced slower and less complete oil uptake. These behavior aligns with findings in other modified cellulose systems, where optimal silanization balances enhanced hydrophobicity and pore preservation, whereas over-modification restricts pore accessibility and oil sorption capacity [19].

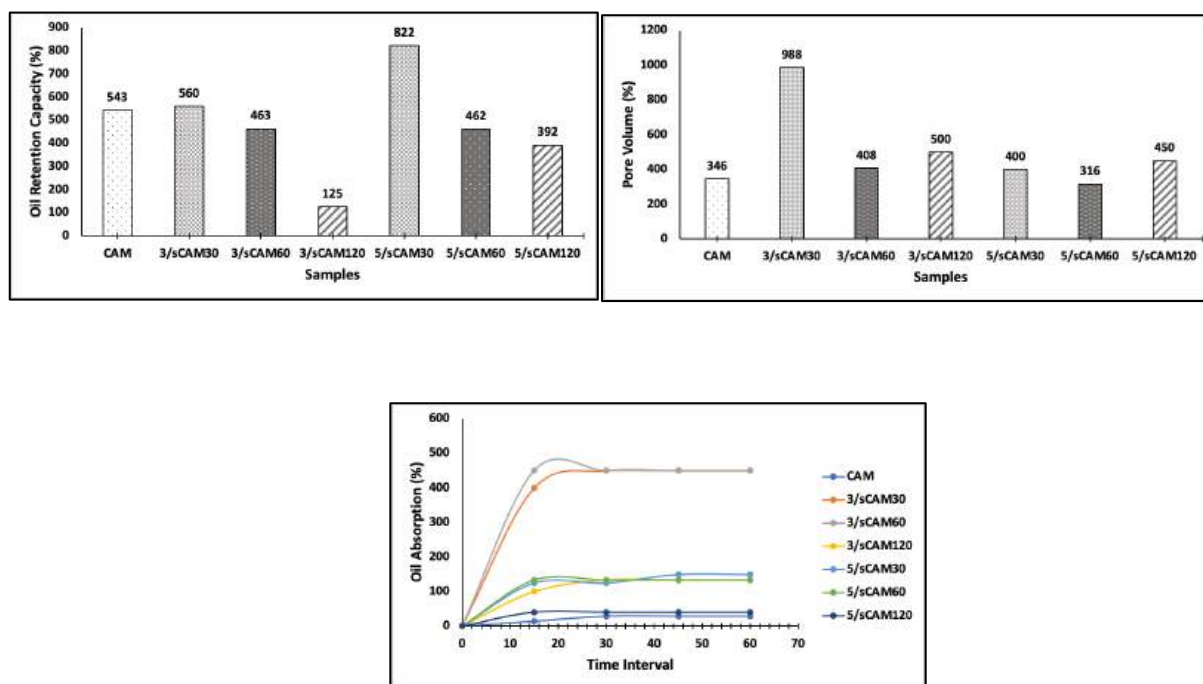


Fig. 5. Oil sorption performance through (a) Oil retention capacity (b) Pore volume and (c) and sCAM

3.5 Oil-water Separation

Owing to their low density, high porosity, and surface hydrophobicity, to examine the oil-water separation and absorption behavior of CAM and sCAM, the samples were dropped on oil-water mixed. The images illustrate in **Fig. 7** shows the capability of Cam and sCAM to separate oil from an oil–water mixture. In **Fig. 7a**, CAM beads exhibit limited ability to selectively absorb oil droplets from the water surface. While the hydrophilic nature of unmodified CAM allows some degree of oil uptake, the beads are also prone to partial water absorption due to the presence of hydroxyl groups on cellulose chains, which reduces their selectivity for oil.

However, **Fig. 7b** demonstrates the superior performance of sCAM in oil–water separation. The silanization of CAM introduces hydrophobic silane groups on the aerogel surface, which enhance oil affinity while repelling water. As a result, sCAM beads effectively extract and retain oil droplets from the water phase, forming aggregated oil-laden beads that float at the water–air interface. The magnified inset highlights the efficient capture of dispersed oil droplets, suggesting that silane modification promotes selective adsorption and prevents water ingress into the aerogel structure [19]. The enhanced performance of sCAM can be attributed to the hydrophobic surface chemistry imparted by silanization, which favors oil sorption and excludes water molecules, and the porous structure of the aerogel, which provides a high surface area for oil uptake [26].

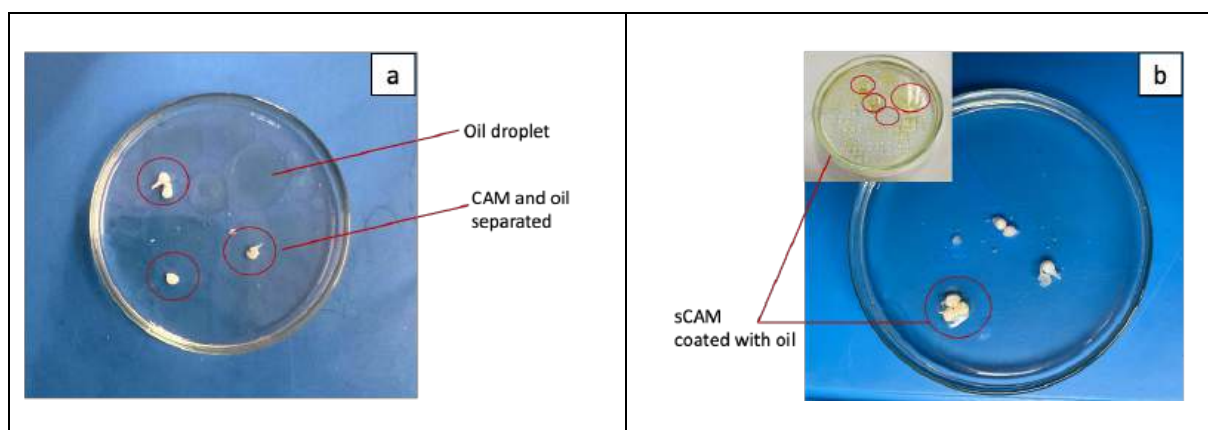
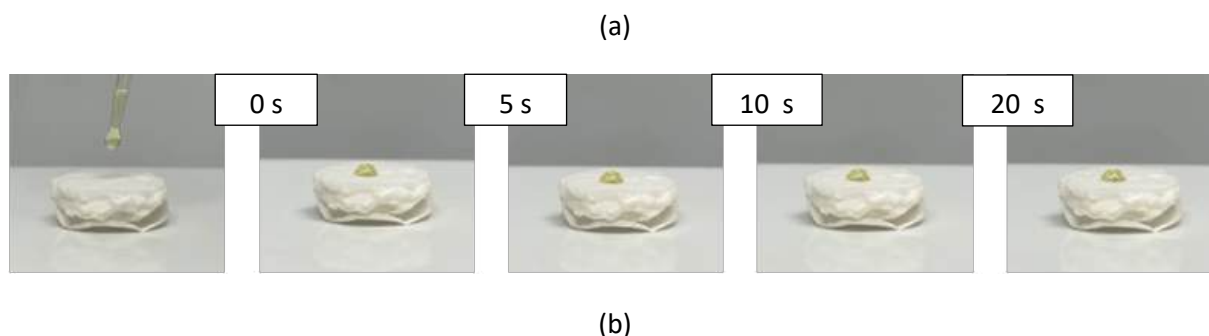


Fig. 7. Oil-water separation of (a) CAM and (b) sCAM

3.6 Contact Angle

Fig. 8 shows the contact angle measurements of cellulose aerogel microbeads (CAM) and (b) silanated cellulose aerogel microbeads (sCAM) at different contact times (0 s, 5 s, 10 s, and 20 s). **Fig. 8a** exhibited rapid droplet spreading, indicative of a highly hydrophilic surface, likely due to the abundance of hydroxyl groups capable of forming hydrogen bonds with water. However, in **Fig. 8b**, the sCAM sample maintained a nearly spherical droplet shape throughout the contact period, demonstrating enhanced hydrophobicity as a result of surface modification with hydrophobic silane moieties, which significantly reduced surface energy and water affinity [13].





3. Conclusion

In this study, cellulose aerogel microbeads (CAM) were successfully fabricated and modified via silanization using trimethoxymethylsilane (TMMS) to produce hydrophobic silanized cellulose aerogel microbeads (sCAM). FTIR confirmed the formation of siloxane bonds, while TGA revealed enhanced thermal stability in sCAM. The silanization process significantly improved oil absorption capacity, pore volume, and oil–water separation efficiency, with 5/sCAM30 showing optimal performance. Contact angle measurements demonstrated the transformation from hydrophilic to hydrophobic surfaces. This environmentally friendly approach produced biodegradable sorbent materials suitable for wastewater treatment and oil spill remediation, supporting sustainability and aligning with the National Biomass Strategy 2020 and United Nations SDG 2030.

Acknowledgement

This research was funded by the Ministry of Higher Education (MOHE) of Malaysia under the Fundamental Research Grant Scheme (FRGS/1/2024/STG05/USIM/02/4) and funding from Universiti Sains Islam Malaysia under grant (PPPI/PTJ/KPI/USIM/18424). The authors also thank Halal Laboratory, Kolej PERMATA Insan, Universiti Sains Islam Malaysia and the Faculty of Science and Technology, Universiti Sains Islam Malaysia for their support in providing instruments and analysis facilities.

References

- [1] El Allaoui, Brahim, Hanane Chakhtouna, Nadia Zari, Hanane Benzeid, Abou el kacem Qaiss, and Rachid Bouhfid. "Superhydrophobic alkylsilane functionalized cellulose beads for efficient oil/water separation." *Journal of Water Process Engineering* 54 (2023): 104015. <https://doi.org/10.1016/j.jwpe.2023.104015>
- [2] Dai, Jiangdong, Zhongshuai Chang, Atian Xie, Ruilong Zhang, Sujun Tian, Wenna Ge, Yongsheng Yan, Chunxiang Li, Wei Xu, and Rong Shao. "One-step assembly of Fe (III)-CMC chelate hydrogel onto nanoneedle-like CuO@ Cu membrane with superhydrophilicity for oil-water separation." *Applied Surface Science* 440 (2018): 560-569. <https://doi.org/10.1016/j.apsusc.2018.01.213>
- [3] Gu, Hongbo, Chong Gao, Xiaomin Zhou, Ai Du, Nithesh Naik, and Zhanhu Guo. "Nanocellulose nanocomposite aerogel towards efficient oil and organic solvent adsorption." *Advanced Composites and Hybrid Materials* 4, no. 3 (2021): 459-468. <https://doi.org/10.1007/s42114-021-00289-y>
- [4] Peng, Min, Yuan Zhu, Hui Li, Kai He, Guangming Zeng, Anwei Chen, Zhenzhen Huang, Tiantian Huang, Lei Yuan, and Guiqiu Chen. "Synthesis and application of modified commercial sponges for oil-water separation." *Chemical Engineering Journal* 373 (2019): 213-226. <https://doi.org/10.1016/j.cej.2019.05.013>
- [5] Tursi, Antonio, Amerigo Beneduci, Francesco Chidichimo, Nicoletta De Vietro, and Giuseppe Chidichimo. "Remediation of hydrocarbons polluted water by hydrophobic functionalized cellulose." *Chemosphere* 201 (2018): 530-539. <https://doi.org/10.1016/j.chemosphere.2018.03.044>
- [6] Etchepare, R., H. Oliveira, A. Azevedo, and J. Rubio. "Separation of emulsified crude oil in saline water by dissolved air flotation with micro and nanobubbles." *Separation and Purification Technology* 186 (2017): 326-332. <https://doi.org/10.1016/j.seppur.2017.06.007>

- [7] Assar, Moein, Sebastien Simon, Geir Humborstad Sørland, and Brian Arthur Grimes. "A theoretical and experimental investigation of batch oil-water gravity separation." *Chemical Engineering Research and Design* 194 (2023): 136-150. <https://doi.org/10.1016/j.cherd.2023.04.029>
- [8] Mishra, Kirti, Samarjeet Singh Siwal, Thandiwe Sithole, Nirankar Singh, Phil Hart, and Vijay Kumar Thakur. "Biorenewable materials for water remediation: the central role of cellulose in achieving sustainability." *Journal of Bioresources and Bioproducts* 9, no. 3 (2024): 253-282. <https://doi.org/10.1016/j.jobab.2023.12.002>
- [9] Yang, Sudong, Lin Chen, Shanshan Wang, and Shuai Liu. "Production of superwetting cellulose II based membranes with excellent oil/water emulsions separation performance." *Industrial Crops and Products* 177 (2022): 114554. <https://doi.org/10.1016/j.indcrop.2022.114554>
- [10] Wang, Tiecheng, Linlong Xing, Muchao Qu, Yamin Pan, Chuntai Liu, Changyu Shen, and Xianhu Liu. "Superhydrophobic polycarbonate blend monolith with micro/nano porous structure for selective oil/water separation." *Polymer* 253 (2022): 124994. <https://doi.org/10.1016/j.polymer.2022.124994>
- [11] El-Gendy, Nour Sh, and Hussein N. Nassar. "Study on the effectiveness of spent waste sugarcane bagasse for adsorption of different petroleum hydrocarbons water pollutants: kinetic and equilibrium isotherm." *Desalination and Water Treatment* 57, no. 12 (2016): 5514-5528. <https://doi.org/10.1080/19443994.2015.1004598>
- [12] Gu, Hongbo, Chong Gao, Xiaomin Zhou, Ai Du, Nithesh Naik, and Zhanhu Guo. "Nanocellulose nanocomposite aerogel towards efficient oil and organic solvent adsorption." *Advanced Composites and Hybrid Materials* 4, no. 3 (2021): 459-468. <https://doi.org/10.1007/s42114-021-00289-y>
- [13] Cerny, Pavel, Petr Bartos, Pavel Kriz, Pavel Olsan, and Petr Spatenka. "Highly hydrophobic organosilane-functionalized cellulose: A promising filler for thermoplastic composites." *Materials* 14, no. 8 (2021): 2005. <https://doi.org/10.3390/ma14082005>
- [14] Kaco, Hatika, Abdul Aziz Md Yunus, Ahmad Amer Mukmin Mohd Radzi, Muhammad Haziq Bahtiar, Muhammad Haikal Honan, Mohd Shaiful Sajab, and Sarani Zakaria. "Oil Water Separation: Inauguration of Cellulose and Chemically Modified Cellulose-rGO via Graphene Oxide Functionalization." (2020).
- [15] Baraka, Farida, Kathirvel Ganesan, Barbara Milow, and Jalel Labidi. "Cellulose nanofiber aerogels: effect of the composition and the drying method." *Cellulose* 31, no. 16 (2024): 9699-9713. <https://doi.org/10.1007/s10570-024-06191-2>
- [16] Parajuli, Prakash, Sanjit Acharya, Julia L. Shamshina, and Nouredine Abidi. "Tuning the morphological properties of cellulose aerogels: an investigation of salt-mediated preparation." *Cellulose* 28, no. 12 (2021): 7559-7577. <https://doi.org/10.1007/s10570-021-04028-w>
- [17] Kaco, Hatika, Sarani Zakaria, Mohd Shaiful Sajab, and Anis Syuhada Mohd Saidi. "Characterization of Aldehyde Crosslinked Kenaf Regenerated Cellulose Film." *BioResources* 10, no. 4 (2015). <https://doi.org/10.15376/biores.10.4.6705-6719>
- [18] Sajab, Mohd Shaiful, Chin Hua Chia, Chi Hoong Chan, Sarani Zakaria, Hatika Kaco, Soon Wei Chook, Siew Xian Chin, and An'Amr Mohamed Noor. "Bifunctional graphene oxide–cellulose nanofibril aerogel loaded with Fe (III) for the removal of cationic dye via simultaneous adsorption and Fenton oxidation." *RSC advances* 6, no. 24 (2016): 19819-19825. <https://doi.org/10.1039/C5RA26193G>
- [19] Nguyen, Dinh Duc, Cuong Manh Vu, Huong Thi Vu, and Hyoung Jin Choi. "Micron-size white bamboo fibril-based silane cellulose aerogel: fabrication and oil absorbent characteristics." *Materials* 12, no. 9 (2019): 1407. <https://doi.org/10.3390/ma12091407>
- [20] Qiu, Jiahao, Xingzhong Guo, Wei Lei, Ronghua Ding, Yun Zhang, and Hui Yang. "Facile preparation of cellulose aerogels with controllable pore structure." *Nanomaterials* 13, no. 3 (2023): 613. <https://doi.org/10.3390/nano13030613>
- [21] Cichosz, Stefan, and Anna Masek. "Cellulose fibers hydrophobization via a hybrid chemical modification." *Polymers* 11, no. 7 (2019): 1174. <https://doi.org/10.3390/polym11071174>
- [22] Vishnoi, Yash, Alok Kumar Trivedi, M. K. Gupta, Harinder Singh, Sanjay Mavinkere Rangappa, and Suchart Siengchin. "Extraction of nano-crystalline cellulose for development of aerogel: Structural, morphological and antibacterial analysis." *Heliyon* 10, no. 1 (2024). <https://doi.org/10.1016/j.heliyon.2023.e23846>
- [23] Ahmadzadeh, Safoura, Angelina Sagardui, David Huitink, Jingyi Chen, and Ali Ubeyitogullari. "Cellulose–Starch Composite Aerogels as Thermal Superinsulating Materials." *ACS omega* 9, no. 50 (2024): 49205-49213. <https://doi.org/10.1021/acsomega.4c05840>
- [24] Herbst, Giulia, Roberto J. Aguado, Quim Tarrés, Marcos L. Corazza, Luiz P. Ramos, Pere Mutjé, and Marc Delgado-Aguilar. "Silane-modified high-yield lignocellulosic fibers as reinforcement of polylactic acid: Enhancement of interfacial adhesion for high-performance biocomposites." *Industrial Crops and Products* 218 (2024): 119027. <https://doi.org/10.1016/j.indcrop.2024.119027>

- [25] Lin, Wensheng, Xiaoyong Hu, Xueqing You, Yingying Sun, Yueqin Wen, Wenbin Yang, Xinxiang Zhang, Yan Li, and Hanxian Chen. "Hydrophobic modification of nanocellulose via a two-step silanation method." *Polymers* 10, no. 9 (2018): 1035. <https://doi.org/10.3390/polym10091035>
- [26] Segneanu, Adina-Elena, Dumitru-Daniel Herea, Gabriela Buema, Ionela Amalia Bradu, Melinda Cepan, and Ioan Grozescu. "Advanced aerogels for water remediation: unraveling their potential in fats, oils, and grease sorption—a comprehensive review." *Gels* 11, no. 4 (2025): 268. <https://doi.org/10.3390/gels11040268>